



Interplay between the reversibility of the inverse magnetocaloric effect and kinetic arrest in Ni-Co-Mn-Sn Heusler alloys

Tapas Samanta^{a,*}, Chris Taake^a, Laila Bondzio^a, Andreas Hütten^a, Luana Caron^{a,b,**}

^a Faculty of Physics, Bielefeld University, PO Box 100131, Bielefeld D-33501, Germany

^b Helmholtz-Zentrum Berlin für Materialien und Energie, Berlin 12489, Germany

ARTICLE INFO

Keywords:

Kinetic arrest
Reversible entropy change
Martensitic phase transition
Strain glass state

ABSTRACT

The nature of martensitic phase transitions and its modification as a function of composition and application of magnetic field have been studied in detail for Ni₄₀Co₁₀Mn₄₀Sn_{10-x}Ga_x ($x=0, 0.3, 0.4$ and 0.5). The phase transition temperature (T_M) increases with increasing x . The kinetic arrest (KA) of the austenitic phase has been observed for $x=0$ and 0.3 , which disappeared for $x>0.3$. The KA results in a decrease in the change of magnetization (ΔM) across T_M . However, the isothermal entropy change ΔS varies almost linearly with $[dT_M/d(\mu_0 H)]^{-1}$ (field-induced shift in T_M) irrespective of the composition variation and thermal cycling. This behavior indicates that the variation of $dT_M/d(\mu_0 H)$ is the dominant factor determining the magnitude of the ΔS rather than ΔM . Consequently, the effect of KA on ΔM has a negligible influence on ΔS in the studied Heusler alloys. The reduced field-sensitivity in T_M associated with the temperature-induced decrease of magnetization in the ferromagnetic austenitic phase leads to a decrease of the thermal hysteresis and an increase of ΔS . As a result, a large reversible ($|\Delta S_{rev}|=21$ J/kg K for $\Delta\mu_0 H=5$ T) has been observed for $x=0.5$, which exceeds previously reported values for Sn-based Heusler alloys.

1. Introduction

The study of the magnetocaloric (MCE) properties in Ni-Mn-based full Heusler alloys is an attractive field of research due to its large inverse MCE originating from a first-order magnetostructural transformation (FOMT) between a weak magnetic martensitic (MP) to a ferromagnetic austenitic phase (AP) [1,2]. For conventional MCE observed around a ferromagnetic-paramagnetic FOMT, the total isothermal entropy change ΔS (MCE parameter) is often expressed as $\Delta S = \Delta S_{lat} + \Delta S_{mag}$ for magnetocaloric materials where the contribution of the electronic entropy change (ΔS_{el}) on ΔS (ΔS_{lat} and ΔS_{mag} represent lattice and magnetic entropy changes, respectively) is considered negligible [3]. A synergistic response of ΔS_{lat} and ΔS_{mag} has been observed for conventional MCE. However, ΔS_{lat} and ΔS_{mag} counteract each other on ΔS for inverse magnetocaloric materials [4–6]. Based on existing literature for Heusler alloys exhibiting an inverse magnetocaloric effect, it is quite obvious that the lattice has a dominant contribution (ΔS_{lat}) to the total ΔS while the ΔS_{el} contribution is relatively small [4–7]. For simplicity, we considered two major contributions to ΔS , i.e., ΔS_{lat} and ΔS_{mag} similar to earlier studies, for describing the

overall behavior of the inverse magnetocaloric effect (by assuming that the contribution of cross coupling terms between lattice, magnetic and electronic degrees of freedom are smaller than the individual contributions [8]). The competing contributions of ΔS_{lat} and ΔS_{mag} to the inverse MCE will reduce the absolute value of ΔS ($\pm\Delta S = |\pm\Delta S_{lat}| - |\mp\Delta S_{mag}|$) compared to what could be obtained if the two contributions behaved synergistically. Concurrently, a large change of magnetization across the martensitic phase transition is desirable for a large ΔS according to Clausius Clapeyron equation ($\Delta S = -\frac{\Delta M}{\Delta T}\Delta\mu_0 H$). The above-mentioned contradictory role of the magnetic contribution is a characteristic feature of the Heusler alloys exhibiting an inverse MCE, and has been examined earlier for Ni-Mn-In and Ni-Mn-In-Co Heusler alloys [4–6].

Kinetic arrest (KA) of the ferromagnetic AP as often observed at the martensitic transformation (AP to MP) of Heusler alloys [9–14] is an additional effect that can also change the magnetic contribution. In fact, KA can reduce the effective ΔM across the martensitic phase transition due to the untransformed AP fraction during cooling in the presence of a magnetic field. The reduction in ΔM therefore is expected to result in a

* Corresponding author.

** Corresponding author at: Faculty of Physics, Bielefeld University, PO Box 100131, Bielefeld D-33501, Germany.

E-mail addresses: tsamanta@physik.uni-bielefeld.de (T. Samanta), lcaron@physik.uni-bielefeld.de (L. Caron).

decrease of ΔS . Earlier studies indicate that the kinetically arrested AP is relatively stable and exhibits a nonergodic, magnetic-glass-like dynamical behavior [15]. As a result, without removing the applied magnetic field and heating it up above the phase transition temperature, it is hardly possible to de-arrest the trapped AP and recover the complete phase transformation.

Although, the KA phenomenon is often observed in ferromagnetic Heusler alloys, the origin of the effect is not properly highlighted in the literature. Recently, Hao *et al.* [16] reported that the existence of a strain-glass (SG) state between the ferromagnetic AP and the weak magnetic MP can result in a KA of the AP. The SG state consists of a frozen disorder in the lattice strain [17–19]. Therefore, the SG transition from ferromagnetic AP is not accompanied with the changes in the average crystal structure [19]. In contrast to the usual martensitic transition between AP and MP (related to a modification of the average crystal structure) exhibiting a pronounced peak in the DSC heat flow curve associated with the latent heat, no thermal peak is expected to be visible in the DSC measurements for a SG to AP transition. It has been extensively studied that the SG transition from AP results in the disappearance of the DSC thermal peak for ferroelastic Ni-Ti nitinol alloys [20]. A similar feature has also been detected in ferromagnetic shape memory Heusler alloys, such as $\text{Ni}_{43}\text{Co}_{12}\text{Mn}_{20}\text{Ga}_{25}$ [21] and $\text{Ni}_{37}\text{Co}_{11}\text{Mn}_{52-x}\text{Sn}_x$ [16]. Although, energetically it is plausible to stabilize a strain glass state and a strain glass transition that can result in the KA of the ferromagnetic AP [16,19]. However, the correlation between the strain glass transition and KA is relatively unexplored for ferromagnetic Heusler alloys and deserves more attention concerning its connection with the functional properties. In the present study, a SG-like state that resulted in KA has been detected for $\text{Ni}_{40}\text{Co}_{10}\text{Mn}_{40}\text{Sn}_{10-x}\text{Ga}_x$ ($x=0$ and 0.3). The effect of KA on the inverse MCE (positive ΔS with application of a magnetic field or during the cooling cycle) and associated reversibility have been examined and discussed.

2. Experimental

A conventional arc-melting procedure under ultra-high purity Ar atmosphere was used to prepare $\text{Ni}_{40}\text{Co}_{10}\text{Mn}_{40}\text{Sn}_{10-x}\text{Ga}_x$ ($x=0, 0.3, 0.4$ and 0.5) samples from the constituent elements of purity better than 99.9%. The samples were placed inside evacuated quartz tubes under partially back-filled Ar ($p \sim 200$ mbar) atmosphere and annealed for 20 hours at 950 °C followed by quenching in cold water. X-ray diffraction (XRD) measurements of the samples at room-temperature were performed in a Philips X'Pert Pro MPD diffractometer using $\text{Cu } K_\alpha$ radiation. The XRD patterns are included in the [Supplementary Information](#). A Quantum Design MPMS 3 magnetometer was used to measure DC magnetization, AC susceptibility and magnetotransport. Following the protocol described by Caron *et al.* [22], the isofield $M(T)$ data measured up to 5 T have been used for calculating ΔS employing the Maxwell relation. A standard four-probe method was employed to carry out the transport measurements. Differential scanning calorimetry (DSC) measurements in the absence of magnetic field were performed using a DSC25 (TA Instruments) with a temperature ramp rate of 10 K/min during heating as well as cooling.

3. Results and discussion

The plot of magnetization as a function of temperature for $\mu_0 H=5$ T is shown in Fig. 1(a) for $\text{Ni}_{40}\text{Co}_{10}\text{Mn}_{40}\text{Sn}_{10-x}\text{Ga}_x$ ($x=0, 0.3, 0.4$ and 0.5), which has been measured following the zero-field-cooled (ZFC), field-cooled (FC) cooling and FC heating protocol. A typical martensitic phase transformation from a weak magnetic MP to a ferromagnetic AP has been observed during heating for all the studied compositions and vice-versa during cooling. The thermal hysteresis (ΔT_{hyst}) between heating and cooling $M(T)$ indicates the first-order nature of the martensitic phase transformation. ΔT_{hyst} progressively increases with decreasing the martensitic phase transition temperature (T_M). This type

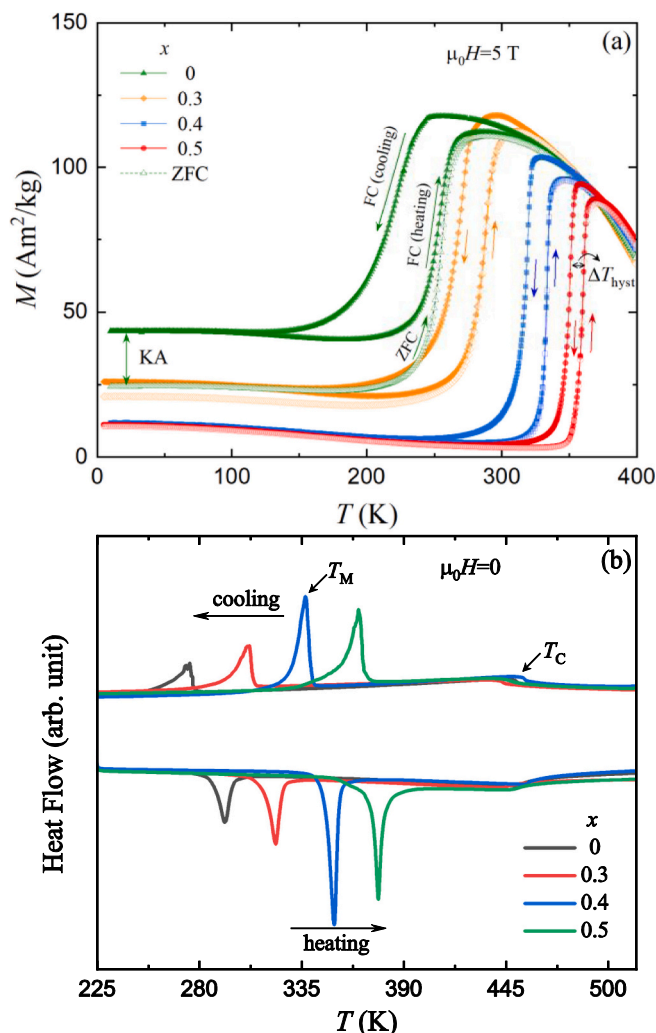


Fig. 1. (a) Magnetization (M) as a function of temperature during ZFC, FC (heating) and FC (cooling) for $\text{Ni}_{40}\text{Co}_{10}\text{Mn}_{40}\text{Sn}_{10-x}\text{Ga}_x$ ($x = 0, 0.3, 0.4$ and 0.5) in the presence of a 5 T magnetic. (b) DSC heat flow curves during heating and cooling for $x=0$ –0.5. The first-order martensitic and second-order ferromagnetic transitions are denoted as T_M and T_C , respectively.

of behavior is associated with the increase of the magnetization in the AP with decreasing T_M as reported earlier for other Heusler alloys [5,6]. A similar increase of ΔT_{hyst} has been observed with the application of a magnetic field for all the studied compositions due to the field-induced decrease of T_M . Below T_M , an irreversibility of the magnetization in the MP has been detected in the $M(T)$ depending on the measurement protocol for the compositions with $x=0$ and 0.3. The FC (both during heating and cooling) magnetization is higher than the ZFC magnetization. This type of increase in M is associated with the KA of a fraction of the ferromagnetic AP during cool-down of the sample through the martensitic phase transformation in the presence of a high magnetic field. This is often observed in Heusler alloys [9–14] and also reported for systems exhibiting a first-order magnetic phase transition such as Ce (Fe, Ru)₂ [15], (Hf, Ta)Fe₂ [23] and FeRh [24]. The KA phenomenon disappears for $x=0.4$ and 0.5 as T_M is shifted to higher temperatures. This feature has been previously reported for Sn-based Heusler alloys [16]. Both the first-order martensitic phase transition and the associated ΔT_{hyst} between heating and cooling curves have been detected in the DSC heat flow curves as shown in Fig. 1(b). Although T_M shifts towards higher temperature with increasing x , the second-order magnetic transition (T_C) from a ferromagnetic to a paramagnetic state within the high-temperature AP is relatively insensitive to Ga concentration. The

increase of T_M with increasing Ga-concentration is likely associated with the substitution of smaller Ga atoms for Sn ($R_{Ga} \sim 0.135$ nm and $R_{Sn} \sim 0.162$ nm) [25] that acts as a positive chemical pressure and mimics the effect of hydrostatic pressure [26].

To understand the possible origin of the KA, the nature of the phase transition during cooling has been examined through DC magnetization, AC susceptibility, DSC and resistivity measurements for $x=0.3$ (the composition is situated at the border above which the KA phenomenon disappears for $x>0.3$). The low-field ($\mu_0H=0.05$ T) DC magnetization curve as a function of temperature shown in Fig. 2(a) exhibits a two-step transition below the ferromagnetic AP: one at T_2 followed by a martensitic transition near T_1 . At low temperature in the MP, a bifurcation between ZFC and FC magnetization curves and a peak at the ZFC branch have been observed for lower applied field (the plot is included in the supplementary material as Fig. S2). This type of bifurcation is often observed for these Sn-based Heusler alloys, resulting from the existence of magnetically inhomogeneous spin-glass-like state [27]. The temperature dependent real-part of the AC susceptibility (χ') is frequency independent between T_2 and T_1 (plotted in Fig. 2(b)), which excludes the possibility of the existence of a spin-glass state. However, the observed peak in $\chi'(T)$ at the MP is frequency dependent as shown in the inset of Fig. 2(b). The shift of the peak position to higher temperatures with increasing frequency indicates an existence of spin-glass-like state with a freezing temperature (corresponding to the peak) that is frequency dependent [27]. A sharp exothermic peak has been detected around T_1 as shown in Fig. 2(c), indicating a martensitic phase transformation. However, no sign for T_2 is observed on the DSC heat flow. Therefore, the transition at T_2 is not connected with the modification in the average crystal structure (the structural changes usually observed for a single ferromagnetic AP to MP transition). It is most likely associated

with a SG transition from the high-temperature ferromagnetic AP as previously reported for Ga- and Sn-based Heusler alloys [16,21]. A large increase in zero-field resistivity (ρ) has been observed around T_1 during cooling associated with the transformation of the low-resistive ferromagnetic AP to the high-resistive martensitic state. However, there is no sudden change in ρ around T_2 . This feature also signifies a SG transition from the high-temperature AP at T_2 . Instead of an increase of ρ below T_2 , as would be expected for the stabilization of the SG state for a higher disorder concentration [17], a monotonic decrease in ρ has been observed until the MP transition starts to occur around T_1 . For the studied composition ($x=0.3$), the disorder concentration of SG is likely dilute enough, so that it barely influences the resistivity (the scattering of conduction electrons is still dominated by the ferromagnetically aligned magnetic moments of the ferromagnetic AP fraction which creates a low-resistive path in the phase matrix) [16] at T_2 . This could be the reason, a further transformation to long-range MP from SG state has been observed around T_1 . Our results indicate that a SG state could exist between the ferromagnetic AP and the long-range MP. In this scenario, the modification of the energy landscape for the stabilization of different phases evolves in such a way that a SG state can be energetically favorable and result in the KA of the AP as indicated earlier [16,19,28].

The KA phenomenon is observed both in the $M(T)$ [shown in Fig. 2 (e)], and in the $\rho(T)$ data measured at a higher field ($\mu_0H=5$ T). The KA of the AP results in an increase of the FC magnetization and concomitantly a reduction of the resistance observed in the FC protocol due to the lower scattering probability of the conduction electrons in the untransformed ferromagnetic AP fraction in the low temperature martensitic matrix. The KA feature is also visible in isothermal $M(\mu_0H)$ curves at 2 K measured cooling the sample down in the presence (i.e., FC) and in the absence (i.e., ZFC) of a magnetic field [shown in Fig. 2(f)].

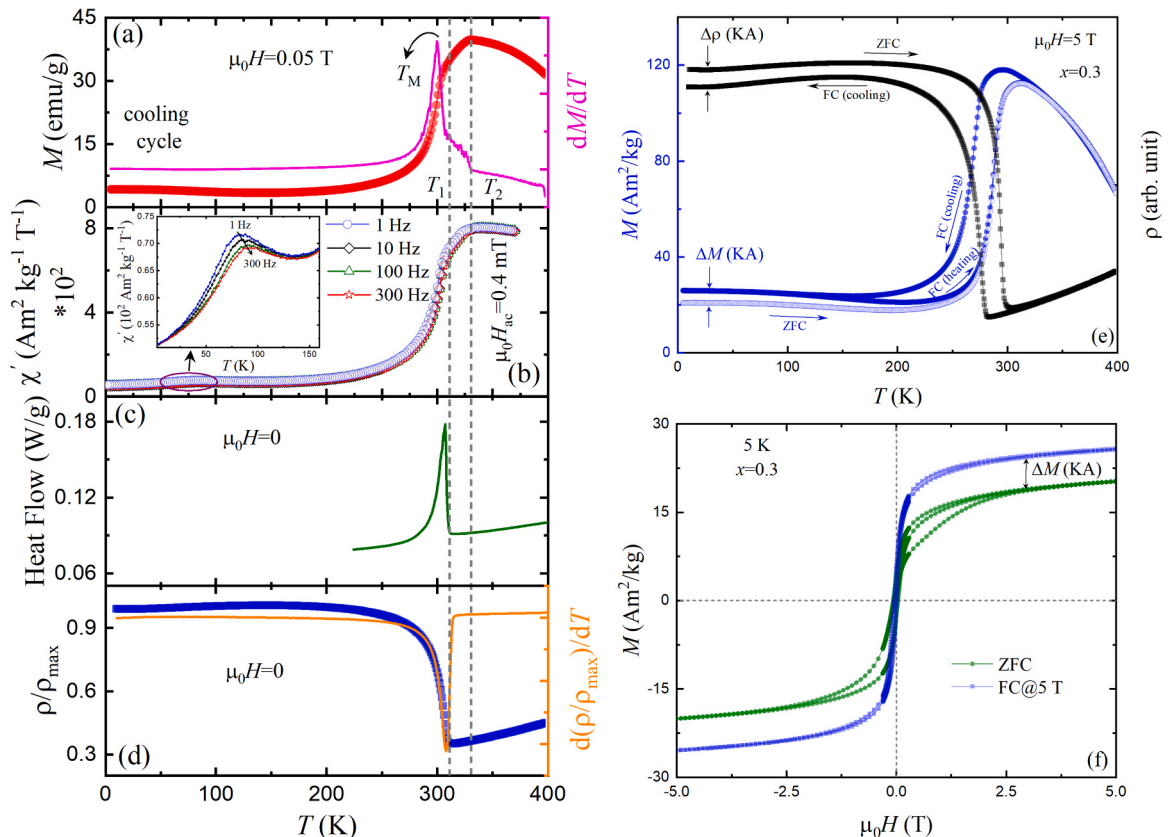


Fig. 2. Temperature dependent cooling curve of (a) DC magnetization, (b) Real-part of AC susceptibility (χ'), (c) DSC heat flow and (d) normalized resistivity for the composition with $x = 0.3$. The corresponding temperature derivative of the (a) magnetization and (d) electrical resistivity at lower temperature is highlighted. The (e) ZFC, FC (heating) and FC (cooling) magnetization (left axis) and the corresponding resistivity (right axis) as a function of temperature for $\mu_0H = 5$ T. The irreversibility between ZFC and FC curves at lower temperature is associated with the kinetic arrest. (f) Magnetization isotherms at 5 K measured following ZFC and FC (the sample was cooled down from above T_M in the presence of a 5 T magnetic field) protocols.

The arrested untransformed ferromagnetic AP fraction leads to a larger saturation magnetization for the FC measurement.

Further, the influence of the KA on the isothermal entropy change (ΔS) has been examined. To estimate the value of ΔS , isofield $M(T)$ data measured at different constant magnetic fields have been used. The temperature and field sweep rates (2 K/min and 100 Oe/s, respectively) for $M(T)$ measurements were exactly the same for all the studied compositions. The plot of $|\Delta S|$ during heating and cooling for $\Delta\mu_0 H=5$ T is shown in Fig. 3. The reversible entropy change ($|\Delta S_{\text{rev}}|$) is represented by the shaded area. The maximum value of $|\Delta S|$ increases with increasing Ga-concentration. The maximum value of $|\Delta S|$ reaches a value of 24.5 J/kg K ($\Delta\mu_0 H=5$ T) during heating for $x=0.5$, resulting from a first-order MP transformation from weak magnetic martensitic to ferromagnetic AP. The observed reversibility in $|\Delta S_{\text{rev}}|$ (21 J/kg K for $\Delta\mu_0 H=5$ T) for $x=0.5$ exceeds the values reported for Sn-based Heusler alloys [(e.g., $|\Delta S_{\text{rev}}|=19.3$ and 18.7 J/kg K for $\Delta\mu_0 H=5$ T reported for Ni₄₃Co₆Mn₄₀Sn₁₁ [29] and Ni₄₁Ti₁Co₉Mn₃₉Sn₁₀ [30], respectively)] and are also comparable with the values reported for the best-known Heusler alloys [(e.g., $|\Delta S_{\text{rev}}|=18.9$ and 16.4 J/kg K for $\Delta\mu_0 H=5$ T reported for Ni_{50.7}Mn_{33.4}In_{15.6}V_{0.3} [31] and Ni₄₆Co₃Mn₃₅Cu₂In₁₄ [32], respectively)]. The maximum value of ΔS decreases for decreasing T_M , which results in a broader $|\Delta S|(T)$ curve and the decrease of the maximum value of $|\Delta S_{\text{rev}}|$ for lower Ga-concentration.

It has been observed that $|\Delta S^{\text{max}}|$ follows a linear dependence with $[dT_M/d(\mu_0 H)]^{-1}$ as shown in Fig. 4. This behavior apparently indicates that the change of magnetization, ΔM , associated with the MP transformation remains invariant according to Clausius Clapeyron equation. From the linear fitting of $|\Delta S^{\text{max}}|$ versus $[dT_M/d(\mu_0 H)]^{-1}$ data, the value of ΔM is estimated as $\Delta M_{\text{average}}=76.91\pm 1.82$ Am²/kg. However, the KA reduces ΔM by about 15 (20 % lower than $\Delta M_{\text{average}}$) and 5 (7 % lower than $\Delta M_{\text{average}}$) Am²/kg for $x=0$ and 0.3, respectively, which can be seen from the plot of $M(T)$ at a 5 T magnetic field. For an unchanged $[dT_M/d(\mu_0 H)]^{-1}$, a 15 Am²/kg decrease of ΔM over 76.91 Am²/kg ($\Delta M_{\text{average}}$) for $x=0$ can reduce the $|\Delta S^{\text{max}}|$ by about 20 %. However, $[dT_M/d(\mu_0 H)]^{-1}$ varies about 70 % [from (3.01 K/T)⁻¹ to (10.22 K/T)⁻¹], resulting in a linear relationship between $|\Delta S^{\text{max}}|$ and $[dT_M/d(\mu_0 H)]^{-1}$. Therefore, the effective reduction in $|\Delta S^{\text{max}}|$ is about 6.6 % [change in $|\Delta S^{\text{max}}|$ (due to KA) = (20 % change in ΔM) / (70 % change in $[dT_M/d(\mu_0 H)]^{-1}$) = 6.6 % change in $|\Delta S^{\text{max}}|$] or 0.5 J/kg K for $x=0$ during cooling. As the field-sensitivity of T_M dominates over the change in

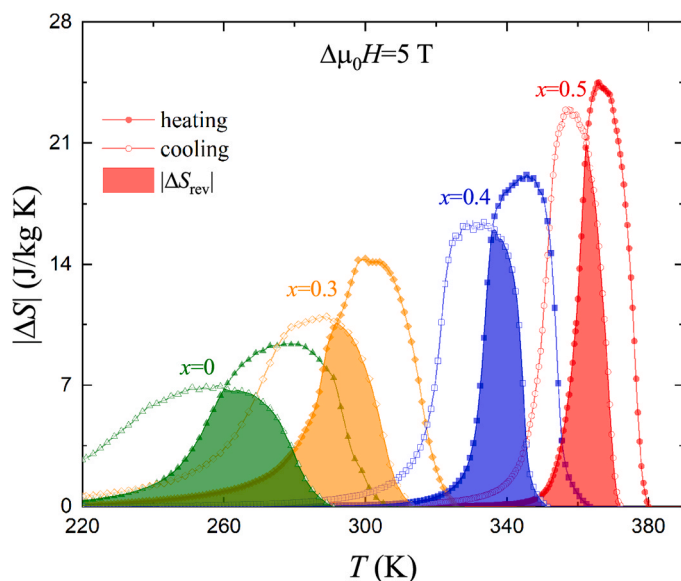


Fig. 3. Entropy change (ΔS) as a function of temperature for Ni₄₀Co₁₀Mn₄₀Sn_{10-x}Ga_x during heating and cooling for a magnetic field change of $\mu_0 H=5$ T. The shaded region indicates the reversible entropy change ($|\Delta S_{\text{rev}}|$).

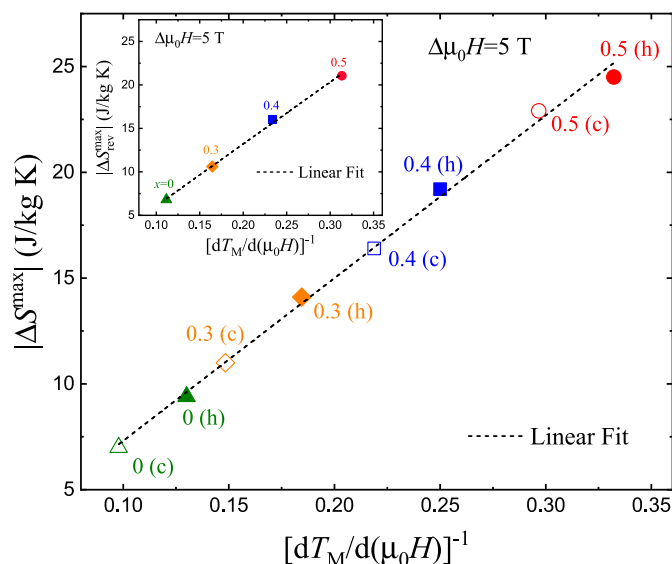


Fig. 4. The variation of maximum entropy change ($|\Delta S^{\text{max}}|$) as a function of $[dT_M/d(\mu_0 H)]^{-1}$ for $\mu_0 H=5$ T. 'h' and 'c' are the abbreviations of heating and cooling, respectively. The number next to the experimental points corresponds to the Ga concentration. Inset: Dependence of maximum reversible entropy change ($|\Delta S_{\text{rev}}^{\text{max}}|$) with $[dT_M/d(\mu_0 H)]^{-1}$ for $\mu_0 H=5$ T.

magnetization in the presently studied system, the observed value of $|\Delta S^{\text{max}}|$ does not reflect the effect of KA. The composition-dependent variation of the maximum reversible entropy change, $|\Delta S_{\text{rev}}^{\text{max}}|$ as a function of $[dT_M/d(\mu_0 H)]^{-1}$ is shown in the inset of Fig. 4. Interestingly, $|\Delta S_{\text{rev}}^{\text{max}}|$ versus $[dT_M/d(\mu_0 H)]^{-1}$ also varies linearly with a slope similar to that observed in the variation of $|\Delta S^{\text{max}}|$.

4. Conclusions

The appearance of a SG-like state between the high-temperature AP and low-temperature MP can result in the KA of the AP as observed for $x=0$ and 0.3. The kinetic arrest phenomena disappear for $x>0.3$, where the intermediate SG state is not observed. A linear dependence of ΔS with inverse $dT_M/d(\mu_0 H)$ has been observed irrespective of composition variations and thermal cycling, indicating that ΔM remains almost constant. However, the experimental results reveal that the variation of $[dT_M/d(\mu_0 H)]^{-1}$ is much larger than the change in ΔM and therefore $[dT_M/d(\mu_0 H)]^{-1}$ has a dominant effect on ΔS . As a result, the KA (which reduces the value of ΔM) has negligible impact on ΔS in the presently studied system. It has been found that the decrease of magnetization in the ferromagnetic austenitic phase by maintaining a large change in ΔM across the MST can improve the value of ΔS associated with the inverse MCE, (due to the decrease of the magnetic entropy change, ΔS_{mag} , which counters the lattice entropy change, ΔS_{lat} , in smaller proportion). In addition, the observed enhancement of the reversibility in $|\Delta S_{\text{rev}}|$ is associated with the reduction of thermal hysteresis across the martensitic phase transition as well as a smaller difference of $dT_M/d(\mu_0 H)$ during heating and cooling, respectively. In turn, if it is possible to maintain a large ΔM with a lower M in the AP (by reducing the separation of T_M and T_C) by fine-tuning the composition, large ΔS and $|\Delta S_{\text{rev}}|$ could be expected for inverse magnetocaloric materials.

CRedit authorship contribution statement

Tapas Samanta: Writing – original draft, Visualization, Investigation, Formal analysis, Conceptualization. **Chris Taake:** Software, Investigation, Formal analysis. **Laila Bondzio:** Investigation. **Andreas Hütten:** Writing – review & editing, Resources, Funding acquisition. **Luana Caron:** Writing – review & editing, Supervision, Funding

acquisition, Conceptualization.

Declaration of Competing Interest

The authors declare the following financial interests/personal relationships which may be considered as potential competing interests: Tapas Samanta, Luana Caron reports financial support was provided by Federal Ministry of Education and Research Berlin Office. If there are other authors, they declare that they have no known competing financial interests or personal relationships that could have appeared to influence the work reported in this paper.

Data availability

Data will be made available on request.

Acknowledgements

This work was carried out in the framework of the Joint Lab BiBer and was supported by the Bundesministerium für Bildung und Forschung (BMBF) joint project DiProMag—Digitalization of a process chain for the production, characterization and prototypical application of magnetocaloric alloys, here the contribution of Bielefeld University: FKZ 13XP5 120B, with the objective of producing magnetocaloric Heusler compounds and ontology development.

Appendix A. Supporting information

Supplementary data associated with this article can be found in the online version at [doi:10.1016/j.jallcom.2024.175145](https://doi.org/10.1016/j.jallcom.2024.175145).

References

- J. Liu, T. Gottschall, K.P. Skokov, J.D. Moore, O. Gutfleisch, Giant magnetocaloric effect driven by structural transitions, *Nat. Mater.* 11 (2012) 620–626.
- T. Krenke, E. Duman, M. Acet, E.F. Wassermann, X. Moya, L. Mañosa, A. Planes, Inverse magnetocaloric effect in ferromagnetic Ni–Mn–Sn alloys, *Nat. Mater.* 4 (2005) 450–454.
- K.A. Gschneidner Jr., Y. Mudryka, V.K. Pecharsky, On the nature of the magnetocaloric effect of the first-order magnetostructural transition, *Scr. Mater.* 67 (2012) 572.
- Z. Li, Y. Zhang, K. Xu, T. Yang, C. Jing, H.L. Zhang, Contribution of entropy changes to the inverse magnetocaloric effect for $\text{Ni}_{46.7}\text{Co}_5\text{Mn}_{33}\text{In}_{15.3}$ Heusler alloy, *Solid State Commun.* 203 (2015) 81–84.
- T. Gottschall, K.P. Skokov, D. Benke, M.E. Gruner, O. Gutfleisch, Contradictory role of the magnetic contribution in inverse magnetocaloric Heusler materials, *Phys. Rev. B* 93 (2016) 184431.
- L. Pfeuffer, T. Gottschall, T. Faske, A. Taubel, F. Scheibel, A.Y. Karpenkov, S. Ener, K.P. Skokov, O. Gutfleisch, Influence of the martensitic transformation kinetics on the magnetocaloric effect in Ni–Mn–In, *Phys. Rev. Mater.* 4 (2020) 111401.
- T. Kihara, X. Xu, W. Ito, R. Kainuma, M. Tokunaga, Direct measurements of inverse magnetocaloric effects in metamagnetic shape-memory alloy NiCoMnIn, *Phys. Rev. B* 90 (2014) 214409.
- L. Mañosa, E. Stern-Taulats, A. Gràcia-Condal, A. Planes, Cross-coupling contribution to the isothermal entropy change in multicaloric materials, *J. Phys. Energy* 5 (2023) 024016.
- V.K. Sharma, M.K. Chattopadhyay, S.B. Roy, Kinetic arrest of the first order austenite to martensite phase transition in $\text{Ni}_{50}\text{Mn}_{34}\text{In}_{16}$: dc magnetization studies, *Phys. Rev. B* 76 (2007) 140401.
- W. Ito, K. Ito, R.Y. Umetsu, R. Kainuma, K. Koyama, K. Watanabe, A. Fujita, K. Oikawa, K. Ishida, T. Kanomata, Kinetic arrest of martensitic transformation in the NiCoMnIn metamagnetic shape memory alloy, *Appl. Phys. Lett.* 92 (2008) 021908.
- A. Lakhani, A. Banerjee, P. Chaddah, X. Chen, R.V. Ramanujan, Magnetic glass in shape memory alloy: $\text{Ni}_{45}\text{Co}_5\text{Mn}_{38}\text{Sn}_{12}$, *J. Phys. Condens. Matter* 24 (2012) 386004.
- J.I. Perez-Landazabal, V. Recarte, V. Sanchez-Alarcos, C. Gomez-Polo, S. Kustov, E. Cesari, Magnetic field induced martensitic transformation linked to the arrested austenite in a Ni–Mn–In–Co, Shape Mem. Alloy, *J. Appl. Phys.* 109 (2011) 093515.
- X. Xu, W. Ito, M. Tokunaga, R.Y. Umetsu, R. Kainuma, K. Ishida, Kinetic arrest of martensitic transformation in NiCoMnAl metamagnetic shape memory alloy, *Mater. Trans.* 51 (2010) 1357.
- R.Y. Umetsu, K. Ito, W. Ito, K. Koyama, T. Kanomata, K. Ishida, R. Kainuma, Kinetic arrest behavior in martensitic transformation of NiCoMnSn, *Metamagnetic shape Mem. Alloy. J. Alloy. Compd.* 509 (2011) 1389.
- M.K. Chattopadhyay, S.B. Roy, P. Chaddah, Kinetic arrest of the first-order ferromagnetic-to-antiferromagnetic transition in $\text{Ce}(\text{Fe}_{0.96}\text{Ru}_{0.04})_2$: formation of a magnetic glass, *Phys. Rev. B* 72 (2005) 180401.
- C. Hao, Y. Wang, J. Wang, C. Liang, D. Duan, D. Wang, S. Yang, X. Song, Kinetic arrest behavior in Ni–Co–Mn–Sn alloys within the phase boundary between martensite and strain glass, *Scr. Mater.* 194 (2021) 113671.
- S. Sarkar, X. Ren, K. Otsuka, Evidence for strain glass in the ferroelastic-martensitic system $\text{Ti}_{50-x}\text{Ni}_{50+x}$, *Phys. Rev. Lett.* 95 (2005) 205702.
- Y. Wang, X. Ren, K. Otsuka, A. Saxena, Evidence for broken ergodicity in strain glass, *Phys. Rev. B* 76 (2007) 132201.
- Y. Wang, X. Ren, K. Otsuka, Strain glass: glassy martensite, *Mater. Sci. Forum* 583 (2008) 67–84.
- Z. Zhang, Y. Wang, D. Wang, Y. Zhou, K. Otsuka, X. Ren, Phase diagram of $\text{Ti}_{50-x}\text{Ni}_{50+x}$: crossover from martensite to strain glass, *Phys. Rev. B* 81 (2010) 224102.
- Y. Wang, C. Huang, J. Gao, S. Yang, X. Ding, X. Song, X. Ren, Evidence for ferromagnetic strain glass in Ni–Co–Mn–Ga Heusler alloy system, *Appl. Phys. Lett.* 101 (2012) 101913.
- L. Caron, N.B. Doan, L. Ranno, On entropy change measurements around first order phase transitions in caloric materials, *J. Phys. Condens. Matter* 29 (2017) 075401.
- R. Rawat, P. Chaddah, P. Bag, P.D. Babu, V. Siruguri, Concentration dependence in kinetic arrest of the first-order magnetic transition in Ta doped HfFe_2 , *J. Phys. Condens. Matter* 25 (2013) 066011.
- P. Kushwaha, A. Lakhani, R. Rawat, P. Chaddah, Low-temperature study of field-induced antiferromagnetic-ferromagnetic transition in Pd-doped Fe–Rh, *Phys. Rev. B* 80 (2009) 174413.
- W.B. Pearson, *The Crystal Chemistry and Physics of Metals and Alloys*, Wiley-Interscience, New-York, 1972.
- T. Yasuda, T. Kanomata, T. Saito, H. Yosida, H. Nishihara, R. Kainuma, K. Oikawa, K. Ishida, K.-U. Neumann, K.R.A. Ziebeck, Pressure effect on transformation temperatures of ferromagnetic shape memory alloy $\text{Ni}_{50}\text{Mn}_{36}\text{Sn}_{14}$, *J. Magn. Magn. Mater.* 310 (2007) 2770–2772.
- J. Sharma, K.G. Suresh, A. Alam, Large exchange bias in Mn–Ni–Sn Heusler alloys: role of cluster spin glass state, *Phys. Rev. B* 107 (2023) 054405.
- Y. Wang, X. Ren, K. Otsuka, A. Saxena, Temperature–stress phase diagram of strain glass $\text{Ti}_{48.5}\text{Ni}_{51.5}$, *Acta Mater.* 56 (2008) 2885–2896.
- Y.H. Qu, D.Y. Cong, S.H. Li, W.Y. Gui, Z.H. Nie, M.H. Zhang, Y. Ren, Y.D. Wang, Simultaneously achieved large reversible elastocaloric and magnetocaloric effects and their coupling in a magnetic shape memory alloy, *Acta Mater.* 151 (2018) 41–55.
- Y.H. Qu, D.Y. Cong, X.M. Sun, Z.H. Nie, W.Y. Gui, R.G. Li, Y. Ren, Y.D. Wang, Giant and reversible room-temperature magnetocaloric effect in Ti-doped Ni–Co–Mn–Sn magnetic shape memory alloys, *Acta Mater.* 134 (2017) 236–248.
- J. Liu, X. You, B. Huang, I. Batashev, M. Maschek, Y. Gong, X. Miao, F. Xu, N. van Dijk, E. Brück, Reversible low-field magnetocaloric effect in Ni–Mn–In-based Heusler alloys, *Phys. Rev. Mater.* 3 (2019) 084409.
- Z. Li, J. Yang, D. Li, Z. Li, B. Yang, H. Yan, C.F. Sánchez-Valdés, J.L.S. Llamazares, Y. Zhang, C. Esling, X. Zhao, L. Zuo, Tuning the reversible magnetocaloric effect in Ni–Mn–In-based alloys through Co and Cu Co-doping, *Adv. Electron. Mater.* 5 (2019) 1800845.